Observation of the Acoustoelectric Effect in Gallium Nitride Micromechanical Bulk Acoustic Filters

Vikrant J. Gokhale, Yonghyun Shim, and Mina Rais-Zadeh
Department of Electrical Engineering and Computer Science
University of Michigan
Ann Arbor, MI, USA
Email: vikrantg@umich.edu

***Abstract*— We report on the experimental verification of the acoustoelectric effect in gallium nitride (GaN) and present a model to describe this effect in GaN thickness-mode bulk acoustic filters. Filters are fabricated using 2.2 µm thick n-type GaN on high resistivity silicon epiwafers obtained from SOITEC. Acoustoelectric effect was observed by applying an electric field parallel to c-axis, the direction of acoustic wave propagation. Improvement in the insertion loss and out-of-band rejection was observed and *Q* amplifications exceeding 240% was achieved. Acoustoelectric effect makes it possible to dynamically tune the frequency response of GaN resonators and filters.**

I. Introduction

Gallium nitride (GaN) is increasingly gaining popularity as a wide bandgap semiconductor material capable of operating in high temperature regimes and at high power levels. This is of significance to monolithic microwave integrated circuit (MMIC) technology. Research into GaN has been mostly focused on its application in microelectronic devices such as high electron mobility transistors (HEMTs), which offer higher power, efficiency and bandwidth than their silicon-based counterparts. However, application of GaN in micro-electromechanical systems (MEMS) has not been much explored. GaN film bulk acoustic resonators (FBARs) have been demonstrated recently by Muller et al [1]. However, the quality factor (*Q*) of the previously reported GaN filters has not been sufficiently high to allow their use in RF circuits or as frequency references. This paper discusses a method that makes it possible to dynamically improve the *Q* of the device using acoustoelectric effect. This effect allows us to amplify the acoustic waves in a thickness mode GaN filter by applying an electric field in the direction of acoustic wave propagation.

The acoustoelectric effect is caused by the interactions between the acoustic phonons and electrons. When the velocity of electrons exceeds the velocity of the acoustic phonons, energy will be transferred from electrons to phonons. This effect can be manifested as an amplification of *Q* in micromechanical resonators. Acoustoelectric effect is easier achieved in piezoelectric semiconductors. GaN exhibits both strong piezoelectricity and possesses large number of intrinsic charge carriers and as such is a strong candidate for the observation of the acoustoelectric effect. In this work, we present measured results that support the theory of *Q* amplification using acoustoelectric effect in GaN micromechanical devices. From a phenomenological perspective, we attempt to explain the acoustoelectric effect in terms of the equivalent electrical model of the GaN filter. The change in the motional and electrical parameters of the model agrees with the theory of acoustoelectric amplification in bulk materials.

II. Acoustoelectric Effect

A. *Acoustoelectric Attenuation*

Historically, the term “acoustoelectric effect” has been associated with the attenuation of a propagating acoustic wave. This attenuation is due to phonon-phonon and electron-phonon interactions in the material. Purely mechanical material losses due to phonon-phonon interactions are well known. The effect of electrons as a loss mechanism was first suggested by Shaposhnikov [2] in 1941, who discussed for the first time the absorption of acoustic wave energy by electrons. This was substantiated by Parmenter [3] in 1953 by observing a DC electric current in the direction of the acoustic wave. This effect was explained in detail in a definitive work by Weinreich [4] who modeled wave-particle drag in a semiconductor. Fundamentally, when an acoustic wave travels through a piezoelectric material, an AC electric field is set up due to the periodically strained regions. Conduction electrons react to this, leading to a spatial redistribution of the carriers. Electrons bunch up at the minima of potential energy which are periodic due to the acoustic wave. Due to the difference in velocities between the electrons and the acoustic wave, there is a phase difference between the electric field and the wave, which causes an energy transfer from the sound wave to the electrons and a resultant attenuation of the acoustic wave [5].

This work was partially supported by the National Science Foundation under Award Number EECS1002036.

B. *Acoustoelectric Amplification*

The converse of this interaction (i.e., acoustoelectric gain) is also possible and was experimentally discovered by Hutson et al, in 1961 [6]. Their work demonstrated the amplification of acoustic waves in photoconductive single crystal cadmium sulphide (CdS) when the velocity of conduction electrons was higher than the sound velocity in the material (Fig. 1). The increased electron drift velocity was attained by increasing the strength of the electric field in the direction of the acoustic wave propagation. The electron-phonon energy transfer was analytically modeled by Spector [7]. This model yields the criterion that the acoustic wave will be amplified when electron drift velocity exceeds the acoustic velocity, causing a crossover from net acoustic loss to net acoustic gain.

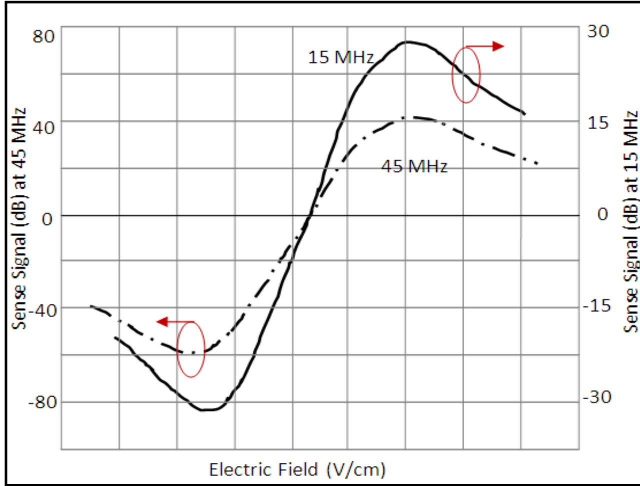

Figure 1. Crossover from acoustic attenuation to acoustic gain in a CdS crystal. After Hutson et al [6].

C. *Current Saturation in Piezoelectric Semiconductors*

An alternate way of looking at the phenomenon of acoustoelectric amplification is purely from the perspective of electrical resistance. Smith [8] showed that piezoelectric semiconductors exhibit non-ohmic behavior upon application of strong pulsed DC signals. In Smith's experiments, the acoustoelectric amplification was verified in CdS by measuring the electric current passing through the CdS crystal as a function of the applied electric field. It was shown that as the electric field increases beyond a certain point, the current exhibits non-ohmic behavior and tends to saturate. The value of the electric field at the transition point from ohmic to non-ohmic region was in agreement with that at the transition from acoustic loss to acoustic gain in CdS.

The current saturation or increase in electrical resistance can be explained from the energy standpoint. As the electric field is increased beyond a critical value, although the total energy of the system increases, due to the electron-to-phonon energy transfer, the increased energy is absorbed by the acoustic wave and does not drive a proportionally greater (or in other words ohmic) electric current. This result was confirmed by Hutson [9].

III. ACOUSTOELECTRIC AMPLIFICATION IN GAN

A. *Acoustoelectric Gain coefficient*

Early experiments using CdS led to a large amount of experimental and analytical work on acoustoelectric amplification. However the inherent processing limitations and the poor quality of CdS crystals available at the time made further research difficult. At the same time, the low electron mobility of CdS made it necessary to use DC voltages on the order of kilovolts in order to measure this amplification (see Eq. 1 for the relation between mobility and amplification). This made practical applications prohibitive in CdS. Research on this effect in bulk semiconductor materials was eventually abandoned due to these practical limitations, and the focus was changed to the more viable surface acoustic wave (SAW) technology [2], [5].

Recently, interest in GaN has been revived due to its use in RF applications as mentioned above. Along with this, analytical treatment by Abdelraheem et al [10] and Mensah et al [11] indicated that GaN is potentially a good candidate for observing amplification of ultrasonic wave using the acoustoelectric effect. Based on the small signal theory originally developed for piezoelectric semiconductors by White [12], Abdelraheem et al [10] presented an expression for the acoustoelectric attenuation (or gain) coefficient α as given by (1).

$$\alpha = \frac{K^2}{2}\frac{\omega_C}{(v_S-\mu E)}\left[1+\frac{{\omega_C}^2{v_S}^2}{(v_S-\mu E)^2\omega^2}\left(1+\frac{\omega^2}{\omega_C\omega_D}\right)\right]^{-1}, (1)$$

where K is the electromechanical coupling coefficient, μ is the electron mobility, v_S is the acoustic velocity, E is the applied DC electric field, ω is the acoustic frequency, ω_C is the dielectric relaxation frequency, and ω_D is the dielectric diffusion frequency [10]. The coefficient α is positive for net acoustic attenuation and negative for net acoustic gain.

Most of the quantities here are dependant solely on the material properties. The only real variable is the value of the applied electric field. The critical term in the expression is the difference between the acoustic velocity and the electron drift velocity, $(v_S-\mu E)$. For net acoustic gain, the electron drift velocity, μE, must exceed the acoustic velocity, v_S. Therefore, a material with high electron mobility is desirable. The value of electron mobility for CdS is approximately 200 cm^2/Vs whereas the theoretically predicted value for GaN is 1500 cm^2/Vs. The highest experimentally measured value for GaN electron mobility is 950 cm^2/Vs (at 300 K) [13], which is still far greater than that of CdS. Therefore, theoretically, GaN is a superior material for exhibiting acoustoelectric amplification at low electric fields. The theoretical models together with the availability of high-quality epitaxially grown thin film GaN on substrate provide us with a strong motivation to study the acoustoelectric effect in GaN at the micro scale and using micromechanical bulk acoustic filters, for the first time.

B. *Q amplification in thickness mode filters*

The device under investigation is a two-port, piezoelectrically transduced, thickness mode, bulk acoustic wave (BAW) filter with electrode configuration as shown in Fig. 2. In this configuration, two acoustic resonators are

coupled through the GaN layer. Therefore, there exist longitudinal standing waves in each individual resonator component and a shear mode wave coupling the two resonators together. The application of a DC bias to one of the RF ports sets up an electric field between the two ports as well as between that port and the bottom (ground) electrode. If acoustoelectric effect prevails with application of sufficient DC bias, both the longitudinal waves and the shear waves should be amplified. The amplification of the shear wave results in lower insertion loss while the amplification of the longitudinal wave brings about a better out-of-band rejection for the filter. They both contribute to the amplification of the filter Q.

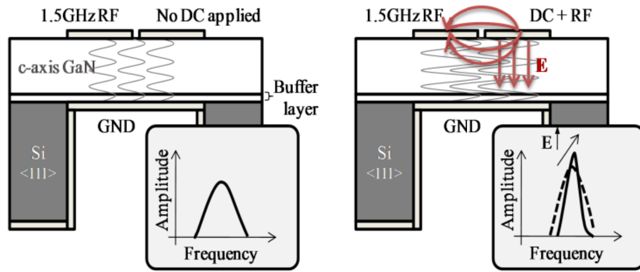

Figure 2. Schematic showing a cross section of the BAW filter and electrode palcement. DC bias is applied to one of the electrodes for acoustoelectric amplification.

IV. FABRICATION

Devices are fabricated using commercially available GaN on silicon epitaxial wafers purchased from SOITECH [14]. The 1.8 µm thick GaN film was grown using molecular beam epitaxy (MBE) on a high resistivity <111> silicon substrate. An additional 0.5 µm thick intermediate buffer layer was required to alleviate the stress mismatch between the substrate and the wurtzite GaN single crystal film. X-ray diffraction (XRD) studies were conducted to study the quality of the GaN film. XRD curves showed a clear peak at a detector angle (2-θ) of 34.51º. The Full Width at Half Maximum (FWHM) of the GaN film is measured to be 0.088º or 316.8 arc seconds, indicating a highly oriented crystalline structure (Fig. 3).

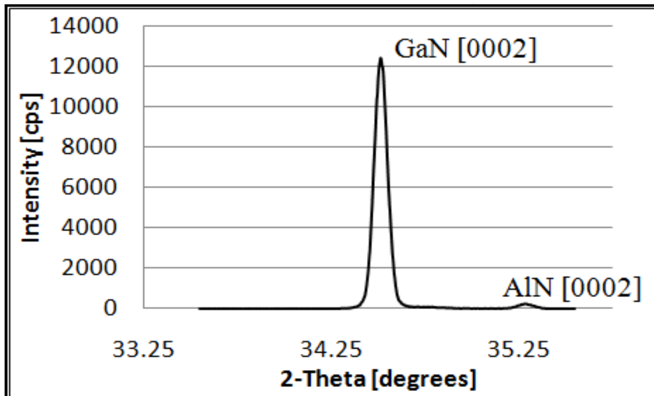

Figure 3. XRD analysis indicates that the peak for [0002] GaN is found at a detector angle of 34.51º. The FWHM for this peak is found to be 0.088ºor 316.8 arc seconds.

We deposited a 50 nm thick silicon dioxide layer on the GaN film to increase the feed-through electrical impedance associated with the semiconducting GaN film. The GaN film was then etched down to form the required patterns using inductively coupled plasma (ICP) etch with chlorine based etch chemistry. Top electrodes consisting of 10 nm Ti and 100 nm Au were patterned using electron beam evaporation and liftoff. The contact pads had a thicker layer consisting of 300 nm Au to reduce the probe to wafer contact resistance. The GaN membranes were released using deep reactive ion etching (DRIE) through the back side of the Si wafer. Backside metallization using 10 nm Ti and 100 nm Au was carried out using sputter deposition for conformal deposition over the DRIE trench profile.

Several designs were studied with different variations in GaN membrane area, aspect ratio, total electroded area, and gap between electrodes. Fig. 4 shows a SEM image of the one of the fabricated devices.

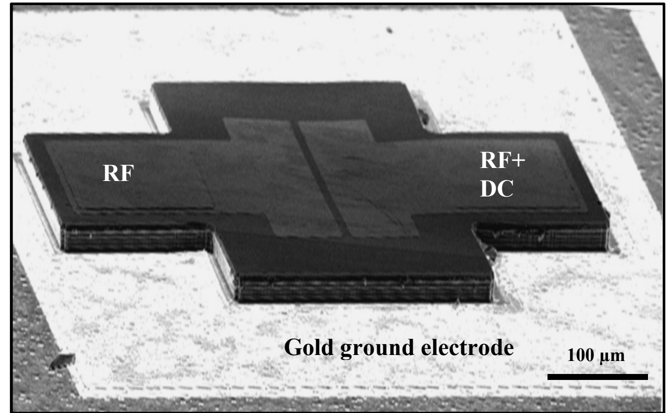

Figure 4: An SEM image of a fabricated GaN BAW filter, indicating electrode placement.

V. MEASURED RESULTS

A. Nominal Frequency Response

The fabricated filters were characterized under atmospheric pressure using a Suss Microtek PM5 probe station, an Agilent N5241A PNA, and Z-probes in the ground-signal-ground (GSG) configuration. For thickness mode filters, the center frequency can be estimated using (2). This expression does not include the effects of the metal electrodes or residual film stress.

$$f_0 = \frac{1}{2t}\sqrt{\frac{E}{\rho}}, \tag{2}$$

where $f_0$is the center frequency, t is the film thickness, E is the effective Young's modulus, and ρ is the density of the material. This gives us a nominal frequency of 1.51 GHz as the resonance of the first thickness mode of the filter. Fig. 5 shows the frequency response of the filter shown in Fig. 4. As shown in Fig. 5, the measured center frequency is 1.503 GHz, which agrees well with the estimated analytical value. The insertion loss of this device is 4.39 dB with a bandwidth of 15 MHz. All devices show a similar center frequency with nominal device to device variation across the wafer.

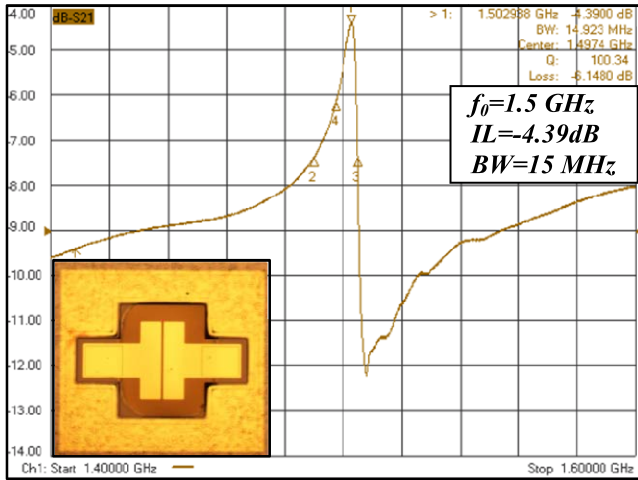

Figure 5. Nominal measured response of the GaN filters together with a microscope image of the device.

B. *Effect of Applied Electric Fields*

Under an applied DC bias to one of the RF ports, the frequency response of the device changes. Fig. 6 shows overlaid responses of a filter at different DC bias levels. We see an increase in the Q and an improvement in the out-of-band rejection level. The insertion loss improves initially by 0.34 dB at 15 V DC, but degrades slightly beyond this.

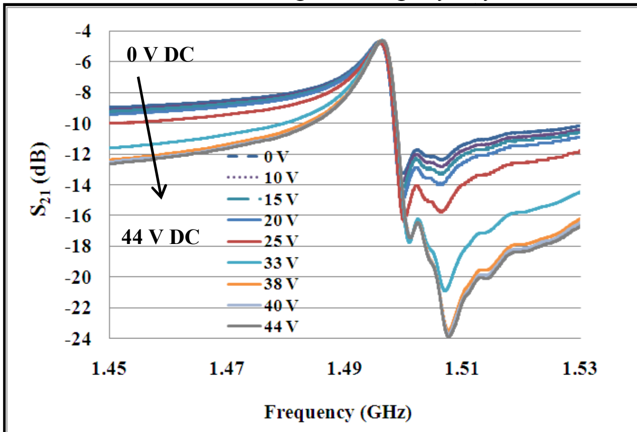

Figure 6. The acoustoelectric amplification of the filter response with an increasing DC bias.

VI. Discussion

A. *Equivalent Electrical Model*

In order to provide a phenomenological explanation for the change in the frequency response of the filter, we modeled the device using the Butterworth-van Dyke (BVD) equivalent electrical model. This method consists of modeling a resonant mechanical component as a passive electrical network with motional resistance, capacitance and inductance. We modify the two- port BVD model slightly to account for the specific characteristics of the fabricated GaN BAW filters. Fig. 7 shows the modified BVD model used here. The model was simulated using Agilent Technology's Advanced Design System (ADS) software.

First, we include a feed-through resistance (R_{feed}) between the two ports to account for the fact that GaN is a semiconductor, and an electrical path between the two ports exists. Second, we add parasitic impedances between the two ports and the bottom ground electrode for a similar reason. The third modification involves the inclusion of a finite resistance between the bottom electrode and electrical ground (R_{GND}). This is due to the fact that the sputter deposition used for backside metallization in a DRIE trench is not ideally conformal at the edges and that the silicon substrate has high resistivity (> 10 kΩ.cm) and does not provide ideal electrical connection to the ground electrode.

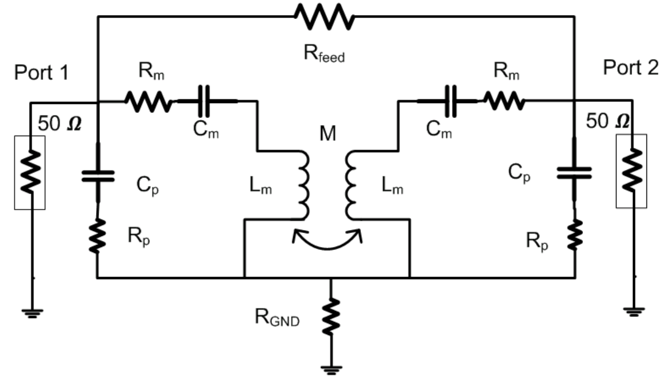

Figure 7. Eqivalent electrical model of the filter using a modified Butterworth van Dyke model.

We matched the measured frequency response and the modeled response for each value of DC voltage in ADS, and extracted the corresponding parameters. As we increase the DC bias, the motional and electrical parameters of the equivalent model undergo changes. These changes follow trends which give us insight into the phenomenon of acoustoelectric gain in a GaN filter. Figs. 8 and 9 show the modeled response compared with the simulated response and the corresponding modified BVD equivalent models at 0 V DC, respectively. Figs. 10 and 11 show the same at 44 V DC. These models are for a filter with an effective electrode area of 180 µm × 90 µm. Similar trends are seen for other device geometries measured across the wafer.

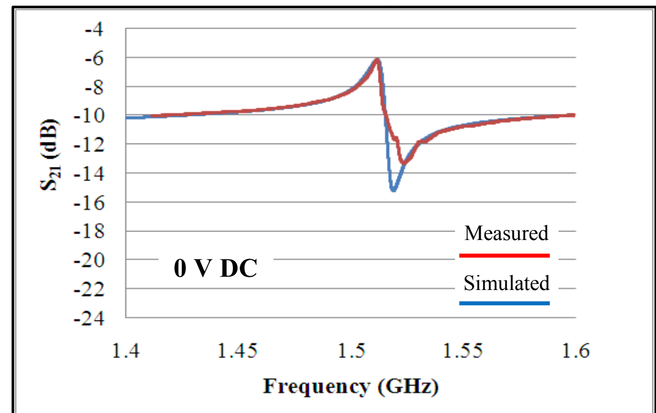

Figure 8. Modeled vs. meausured response of the filter response at 0 V DC.

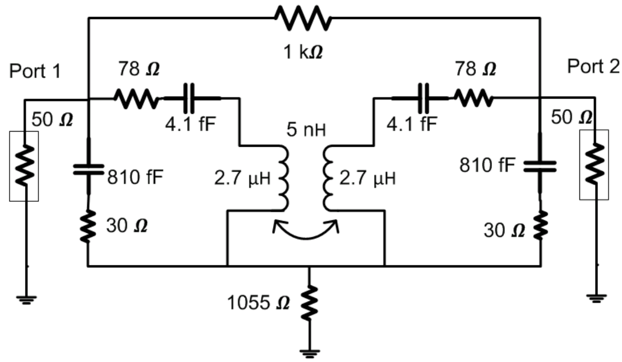

Figure 9. Equivalent model for the filter at 0 V DC

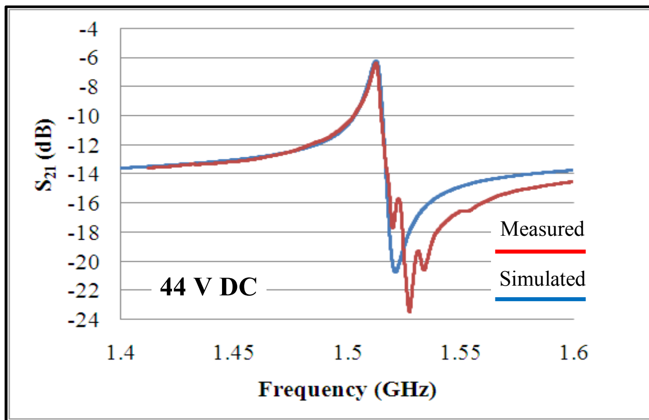

Figure 10. Modeled vs. measured response of the filter at 44 V DC.

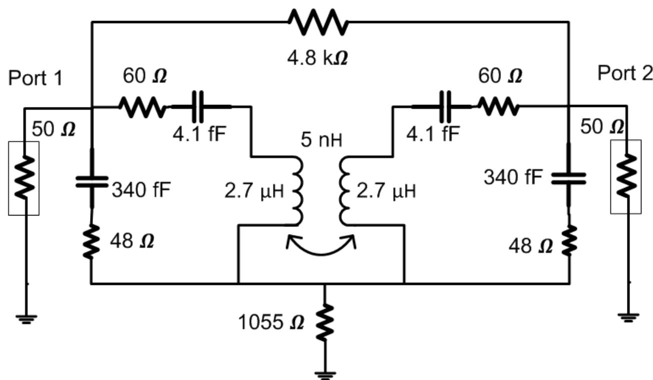

Figure 11. Equivalent model for the filter at 44 V DC.

B. *Motional Impedance*

The motional impedance of the resonator components in the filter decreases with an increase in the DC bias. The motional resistance (R_m) is a measure of the losses due to intrinsic energy dissipation mechanisms in the material. By applying a DC bias, and transferring energy from the electric field to the acoustic wave via the acoustoelectric electron-phonon interaction, we are supplying additional energy to the acoustic domain to offset the material losses dominated by the phonon-phonon interactions. Hence we should expect that acoustoelectric gain be accompanied by a decrease in the motional impedance, and this is supported by the matched BVD model.

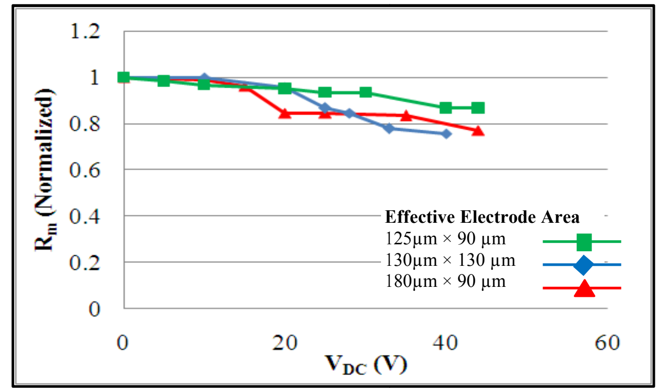

Figure 12. Normalized trends for three device geometries showing decrease in motional impedance with increasing DC bias.

Fig. 12 shows the trend of R_m with increasing DC voltage for three device geometries, normalized with respect to nominal values. The reduction in motional impedance is a clear indication of acoustoelectric amplification. Measured results show that the trend for insertion loss does not perfectly agree with this trend over the entire DC voltage range. The insertion loss improves by 0.34 dB initially reaching its minima at 15 V DC, but then degrades slightly with application of larger DC biases.

C. *Feed-through Resistance*

An electrical feed-through path exists between the ports because of the semiconducting nature of the GaN film. As we increase the DC bias, we see the feed-through resistance increase by up to five times its original value. Fig. 13 shows the normalized trends for increase in R_{feed} with DC bias. To explain this trend, we refer to the current saturation phenomenon described previously, that accompanies acoustoelectric amplification. Beyond the critical electric field, the increasing DC field no longer drives a proportional ohmic current through the material as electrical energy is transferred to the acoustic domain. This current saturation can also be viewed as an increase in the effective electrical resistance of the material, and explains the large increase in the feed-through impedance. The increased feed-through impedance results in improved out-of-band rejection.

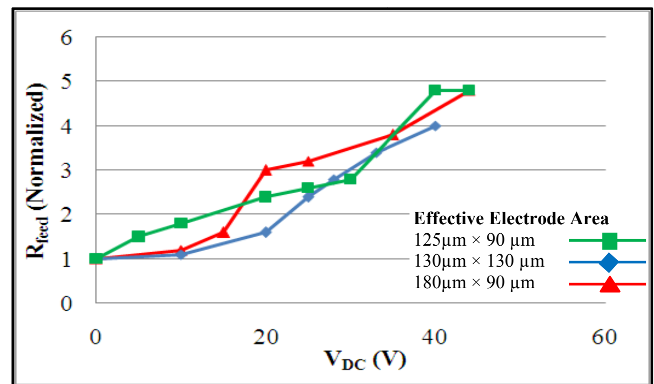

Figure 13. Normalized trends showing increase in feedthrough impedance with increasing DC bias.

D. Port Parasitic Impedances

The parasitic impedances of the resonator components from the input/output ports to ground increase with increasing DC bias. The same argument used for the increasing feed-through resistance can be applied here. Electrical impedances to the ground port increases as the longitudinal acoustic waves are amplified. The increased parasitic impedance also results in increased out-of-band rejection for the filter. Fig. 14 shows the trend for port parasitic impedance (Z_p) as a function of DC bias. The increase in both Z_p and R_{feed} due to acoustoelectric gain thus contributes to the improvement in the response of the filter.

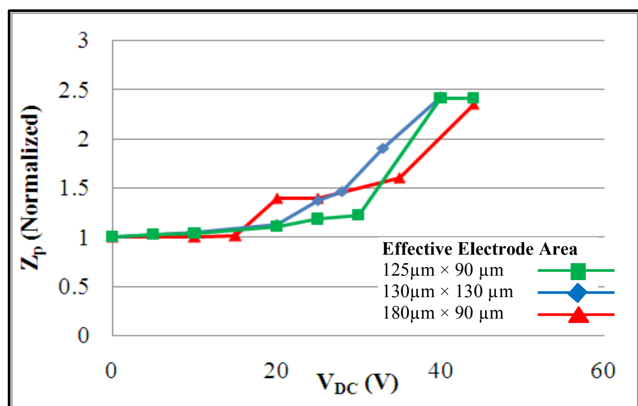

Figure 14. Normalized trends showing increase in parasitic impedance with increasing DC bias.

E. Q Amplification

The amplification of the filter Q is the most tangible result from the measurements. For the same device discussed above, the measured Q increases to 240% of its original value. Fig. 15 shows the normalized trends for Q as a function of DC voltage for three devices with varying geometry. Improvement of motional impedance and out-of-band rejection both contribute to the increase in quality factor. Fig. 15 demonstrates an important result, which is well supported by theory and analytical modeling.

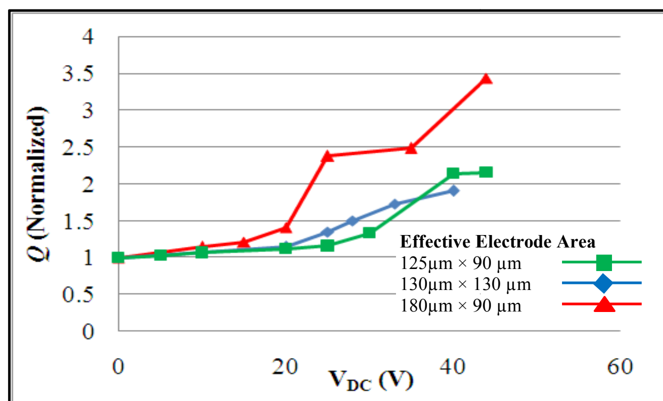

Figure 15. Normalized trends showing increase in Q with increasing DC bias.

VII. Conclusions

This work experimentally demonstrates acoustoelectric amplification in GaN. We have shown an increase in measured Q by 240% of its original value. The acoustoelectric effect is modeled from a phenomenological perspective as a change in the equivalent parameters of the GaN filter. Along with fundamental insights into the mechanisms of this phenomenon, the methodology used for the experiment lends itself easily to making practical devices employing this effect. Acoustoelectric gain can be used to dynamically tune the frequency response of GaN resonators and filters by changing the Q, insertion loss and bandwidth of the device by applying a DC bias. In addition, GaN based resonant sensors with tunable dynamic range and sensitivity can be designed using this effect.

Acknowledgment

The authors would like to thank the staff at the Lurie Nanofabrication Facility at the University of Michigan for assistance with fabrication, and Roozbeh Tabrizian from Georgia Tech for helpful discussion.

References

[1] A.Muller et al, "6.3-GHz Film Bulk Acoustic Resonator structures based on a GaN/Silicon thin membrane," IEEE Electron Device Letters, Vol.30, No.8, pp.799-801, 2009

[2] Yu. Gulyaev and F. S. Hickernell, “Acoustoelectronics: History, present state, and new ideas for a new era” Acoustical Physics, Vol.5, No.1, pp. 81–88, 2005

[3] R.H. Parmenter, “The Acousto-electric effect”, Phys. Rev., Vol.89, No.5, pp.990-998, 1953

[4] G. Weinreich, T.M. Sanders Jr. and H.G. White, “Acoustoelectric effect in n-type Germanium,” Phys. Rev, Vol.114, No.1, pp.33-44, 1959

[5] V.E. Heinreich, “Studies of the acoustoelectric effect, ultrasonic attenuation and trapping in Cadmium Sulphide,” Doctoral thesis, University of Michigan, 1967.

[6] A.R. Hutson, J.H.McFee and D.L.White, “Ultrasonic amplification in CdS,” Phys. Rev. Lett., Vol.7, No.6, pp.237-240,1961

[7] H.N. Spector, “Amplification of acoustic waves through interaction with conduction electrons” Phys. Rev, Vol.127, No.4, pp. 1084-1090, 1962

[8] R. W. Smith, “Current saturation in piezoelectric semiconductors,” Phys. Rev. Letters, Vol. 9, pp. 87-90, 1962.

[9] A.R. Hutson, “Acoustoelectric explanation of non-ohmic behaviour in piezoelectric semiconductors and bismuth,” Phys. Rev. Letters, Vol. 9, No.7, pp.296-298, 1962

[10] S. K. Abdelraheem, D. P. Blyth and N. Balkan, “Amplification of ultrasonic waves in bulk GaN and GaAlN/GaN heterostructures”, Physica Status Solidi. (a), Vol.185, No.2, pp. 247-256, 2001

[11] S. Y. Mensah, N. G. Mensah, V. W. Elloh, G. K. Banini, F. Sam and F. K. A. Allotey, “Propagation of ultrasonic waves in bulk gallium nitride (GaN) semiconductor in the presence of high-frequency electric field”, Physica E, Vol.28, pp. 500-506, 2005

[12] A.R. Hutson and D.L. White, “Elastic wave propagation in piezoelectric semiconductors,” J. Appl. Phys. Vol. 33, No.1, pp. 40-47, 1962

[13] J.H. Edgar, S. Strite, I. Aksaki, H. Amano and C. Wetzel, Properties, Processing and Applications of Gallium Nitride and Related Semiconductors, INSPEC, IEEE, 1999

[14] http://www.soitec.com/picogiga